

# 2nd-order Wave Kinematics Within HydroDyn

## Implimentation

Eungsoo Kim, Andrew Platt, and Jason Jonkman

Thursday 28<sup>th</sup> August, 2014

## Table of Contents

|          |  |           |
|----------|--|-----------|
| <b>1</b> | <b>Overview</b>  | <b>1</b>  |
| <b>2</b> | <b>Synthesis of Directional Waves</b>  | <b>2</b>  |
| 2.1      | Double Summation Method  | 2         |
| 2.2      | Single Summation Method  | 3         |
| 2.3      | Equal Energy Method  | 4         |
| 2.3.1    | Frequency Independent spreading function, $D(\theta)$                            | 4         |
| 2.3.2    | Frequency dependent spreading function, $D(\omega, \theta)$                      | 5         |
| <b>3</b> | <b>Second-order directional wave theory</b>                                      | <b>6</b>  |
| 3.1      | Boundary value problem formulations  | 6         |
| 3.1.1    | Bottom Boundary Condition(BBC)   | 6         |
| 3.1.2    | Kinematics Free Surface Boundary Condition(KFSBC)                                | 6         |
| 3.1.3    | Dynamic Free Surface Boundary Conditions(DFSBC)                                  | 7         |
| 3.1.4    | Combined Free Surface Boundary Condition(CFSBC)                                  | 7         |
| 3.2      | Solution of the Boundary Value Problem   | 7         |
| 3.2.1    | First-Order Solution   | 8         |
| 3.2.2    | Second-Order Solution  | 9         |
| 3.3      | Validity of the Second-order Wave theory   | 10        |
| <b>4</b> | <b>Second-Order Wave Kinematics</b>  | <b>11</b> |
| 4.1      | Wave Surface Elevation   | 12        |
| 4.2      | Wave Particle Velocity   | 12        |
| 4.2.1    | First-Order  | 12        |
| 4.2.2    | Second-Order   | 12        |
| 4.3      | Wave Particle Acceleration   | 13        |
| 4.3.1    | First-Order  | 13        |
| 4.3.2    | Second-Order   | 13        |
| 4.4      | Dynamic Pressure   | 14        |
| 4.4.1    | First-Order  | 14        |
| 4.4.2    | Second-Order (only second-order potential term)                                  | 14        |
| 4.5      | Properties of Quadratic Transfer Function  | 14        |
| 4.5.1    | Symmetry of QTF  | 14        |
| 4.5.2    | Singularity of QTF   | 15        |
| <b>5</b> | <b>Numerical Simulation of Second-Order Wave Kinematics</b>                      | <b>20</b> |
| 5.1      | Limitation of Second-Order Wave Theory   | 20        |
| 5.2      | Sampling Theorem and additional requirement of cut-off frequency, $\omega_{cut}$ | 22        |
| 5.3      | Numerical Simulation using Inverse Fast Fourier Transform(IFFT)                  | 22        |
| 5.3.1    | Sum-Frequency Interaction  | 24        |
| 5.3.2    | Difference-Frequency Interaction   | 24        |
|          | <b>Bibliography</b>  | <b>25</b> |

## List of Figures

|            |  |    |
|------------|--|----|
| Figure 1.  | Transfer function for $\eta^{2\pm}$ ( $\omega > 0$ ): unidirectional wave( $\theta_n = \theta_m = 0$ ) . . . . .                     | 14 |
| Figure 2.  | Transfer function for $\phi^{2\pm}$ ( $\omega > 0$ ) at MSL( $h = 20m$ ): unidirectional wave( $\theta_n = \theta_m = 0$ ) . . . . . | 15 |
| Figure 3.  | Transfer function for $u_x^{2\pm}$ ( $\omega > 0$ ) at MSL( $h = 20m$ ): unidirectional wave( $\theta_n = \theta_m = 0$ ) . . . . .  | 15 |
| Figure 4.  | Transfer function for $u_z^{2\pm}$ ( $\omega > 0$ ) at MSL( $h = 20m$ ): unidirectional wave( $\theta_n = \theta_m = 0$ ) . . . . .  | 16 |
| Figure 5.  | Transfer function for $a_x^{2\pm}$ ( $\omega > 0$ ) at MSL( $h = 20m$ ): unidirectional wave( $\theta_n = \theta_m = 0$ ) . . . . .  | 16 |
| Figure 6.  | Transfer function for $a_z^{2\pm}$ ( $\omega > 0$ ) at MSL( $h = 20m$ ): unidirectional wave( $\theta_n = \theta_m = 0$ ) . . . . .  | 17 |
| Figure 7.  | Transfer function for $p^{2\pm}$ ( $\omega > 0$ ) at MSL( $h = 20m$ ): unidirectional wave( $\theta_n = \theta_m = 0$ ) . . . . .    | 17 |
| Figure 8.  | Transfer function $K_{nm}^{\pm}$ including $\omega = 0$ . . . . .  | 18 |
| Figure 9.  | Transfer function $B_{nm}^{\pm}$ including $\omega = 0$ . . . . .  | 18 |
| Figure 10. | The sum and difference interaction of the wavenumber vectors . . . . .   | 19 |
| Figure 11. | Different criteria for $ka$ as a function of $kd$ . . . . .  | 21 |
| Figure 12. | Second-order wave frequency matrix: Sum-frequency interaction . . . . .  | 23 |
| Figure 13. | Second-order wave frequency matrix: difference-frequency interaction . . . . .   | 23 |

## List of Tables

## 1 Overview

In many engineering applications, especially in deep water, when hydrodynamic loads are to be considered on structures, waves are modeled as long-crested and generated as an irregular sea surface elevation process using linear Airy wave theory and associated kinematics. However, to generate realistic wave fields in shallow water, it is essential to account for both wave directionality and nonlinearity, which is achieved by employing the directional irregular second-order wave modeling approach of Sharma and Dean [1]. Using wave steepness as a perturbation parameter, Stokes [2] provided solutions for the analysis of regular waves. In Stokes study, only the sum frequencies of first-order waves are considered. For irregular waves, both sum- and difference-frequency interactions up to second order are considered. The second-order wave solutions for infinite water depth including the contribution of the difference frequencies were provided by Longuet-Higgins et al. [3]; Sharma and Dean [1] extended the theory for infinite water depth to intermediate water depths.



## 2 Synthesis of Directional Waves

In irregular waves, this is usually described with a directional spectrum or spreading function, similar to a frequency spectrum. It is assumed that the total spectrum can be defined as:

$$S(\omega, \theta) = S(\omega)D(\omega, \theta) \quad (2.1)$$

where  $(\omega)$  is the frequency spectrum, independent of the direction of the waves, and  $D(\omega, \theta)$  is the directional spectrum, which is a function of frequency,  $\omega$  as well as wave direction,  $\theta$ .

### 2.1 Double Summation Method

The most intuitive method for the generation of deterministic waves is to use the double summation method. The basic double summation model for directional waves is a discrete version of the standard double integral equation for the wave elevation of a random sea with continuous distribution of energy over frequency and angle of propagation. It is given by

$$\eta(\vec{x}, t) = Re \left[ \sum_{n=1}^N \sum_{m=1}^M A_{nm} \exp[i(\omega_n t - \vec{k}_{nm} \cdot \vec{x})] \right] \quad (2.2)$$

where,  $\vec{x} = (x, y)$  is a point on the horizontal  $x$ - $y$  plane;  $A_{nm} = a_{nm} \exp(i\varepsilon_{nm})$ ;  $\omega_n$  is the angular frequency;  $\theta_m$  is the wave direction;  $\varepsilon_{nm}$  is the wave phase, which is uniformly distributed between  $[0, 2\pi]$ ;  $\vec{k}_{nm} = (|\vec{k}_{nm}| \cos \theta_m, |\vec{k}_{nm}| \sin \theta_m)$  is the wave number;  $N$  is the total number of frequencies considered; and  $M$  is the total number of wave directions. Also,  $a_{nm}$  are the component spectral amplitudes, which are calculated as follows:

$$a_{nm} = \sqrt{2S(\omega_n, \theta_m)\Delta\omega\Delta\theta} \quad (2.3)$$

The wave field is thus a superposition of  $M$  two-dimensional wave trains propagating in  $M$  different directions with each individual wave train.

Although this double summation model has been used quite extensively for directional wave simulation, several researchers (Forristall [4]; Lambrakos [5]; Pinkster [6]) have reported two basic problems, which are that the resultant wave field is neither ergodic nor spatially homogeneous for finite values of  $N$  and  $M$ , regardless of the record length used. As pointed out by Jefferys [7], these effects are caused by artificial phase locking in any particular realization due to components traveling in different directions with identical frequencies. The wave energy in any one frequency band will therefore typically vary over space from approximately 0 to 4 times its average value regardless of how many directions are used.

The problem can be illustrated by derivation of the cross spectrum between the wave elevations at two spatially separated points. Waves of different frequencies cannot interact linearly so it is safe to consider one frequency in isolation; dropping the subscript, the  $n^{th}$  frequency of the Eq.2.2 contributes to the surface elevation according to Eq.2.4

$$\eta(\vec{x}, t, \omega) = \sum_{m=1}^M a_m \cos(\omega t - \vec{k} \cdot \vec{x} + \varepsilon_m) \quad (2.4)$$

The cross spectrum between the wave elevations at points  $\vec{x}_p = (x_p, y_p)$  and  $\vec{x}_q = (x_q, y_q)$  is denoted by  $S_{pq}(\omega)$ ; it is the Fourier transform of the cross correlation  $R_{pq}(\tau)$  between the two signals at the two points.

$$R_{pq}(\tau) = \lim_{T \rightarrow \infty} \frac{1}{T} \int_0^T \eta(\vec{x}_p, t) \eta(\vec{x}_q, t + \tau) dt \quad (2.5)$$

$$S_{pq}(\omega) = \frac{1}{2\pi} \int_{-\infty}^{\infty} R_{pq}(\tau) \exp(-i\omega\tau) d\tau \quad (2.6)$$

Jefferys(1987) showed that the cross spectrum  $S_{pq}(\omega)$  can be evaluated by the following discrete double summation:

$$S_{pq}(\omega) = \frac{1}{2} \sum_{n=1}^M \sum_{m=1}^M a_n a_m \exp(i(\vec{k}_n \cdot \vec{x}_p - \vec{k}_m \cdot \vec{x}_q + \varepsilon_n - \varepsilon_m)) \quad (2.7)$$

The real part and imaginary part of  $S_{pq}$  are called co-spectrum and quad-spectrum, respectively. This equation can be written in terms of 1) the target cross spectrum and 2) an unwanted interaction component introduced by the phase locked waves.

$$S_{pq}(\omega) = \underbrace{\frac{1}{2} \sum_{m=1}^M a_m^2 \exp(i(\vec{k}_m \cdot (\vec{x}_p - \vec{x}_q)))}_{\text{target}} + \underbrace{\frac{1}{2} \sum_{n=1}^M \sum_{\substack{m=1 \\ m \neq n}}^M a_n a_m \exp(i(\vec{k}_n \cdot \vec{x}_p - \vec{k}_m \cdot \vec{x}_q + \varepsilon_n - \varepsilon_m))}_{\text{interaction}} \quad (2.8)$$

If  $\vec{x}_p$  and  $\vec{x}_q$  are the same point, this expression yields the auto spectrum  $S_{pp}(\omega)$  as following

$$S_{pp}(\omega) = \underbrace{\frac{1}{2} \sum_{m=1}^M a_m^2}_{\text{target}} + \underbrace{\frac{1}{2} \sum_{n=1}^M \sum_{\substack{m=1 \\ m \neq n}}^M a_n a_m \cos(\vec{x}_p \cdot (\vec{k}_n - \vec{k}_m) + \varepsilon_n - \varepsilon_m)}_{\text{interaction}} \quad (2.9)$$

The interaction terms in Eqs.2.8 and 2.9 make the wave field generated by the double summation method neither ergodic nor spatially homogeneous. Only way to effectively eliminate the interaction term is to increase the length of a realization by decreasing  $\Delta\omega$  or to be averaged over many realization.

## 2.2 Single Summation Method

Alternatively, a single summation method with only one direction per each frequency component reproduces all desirable feature of the double summation method but avoids ergodicity problem. This synthesis method will produce a spatially homogeneous wave field because all cross-product terms will average to zero regardless of the direction of propagation of each component. The single summation method is defined by

$$\eta(\vec{x}, t) = \text{Re} \left[ \sum_{n=1}^{NM} A_n \exp(i\omega'_n t - i|\vec{k}_n|(x \cos \theta_n + y \sin \theta_n)) \right] \quad (2.10)$$

The complex amplitudes,  $A_n$  are given by

$$A_n = \left( \sqrt{2S(\omega'_n, \theta_n) \Delta\omega \Delta\theta} \right) \exp(i\varepsilon_n) \quad (2.11)$$

For any specified time step  $\Delta t$  and the length of simulation  $T_{max}$ , the required frequency interval  $\Delta\omega$  can be obtained by

$$\Delta\omega = \frac{2\pi}{T_{max}} = \frac{2\pi}{N\Delta t} \quad (2.12)$$

In each frequency band  $\Delta\omega$ , the directional spreading function is calculated for  $M$  wave directions. There are thus  $M$  sub-frequencies within each frequency band  $\Delta\omega$ , each corresponding to a different wave spreading angle. The sub-frequencies are given by

$$\omega'_n = (n-1) \frac{\Delta\omega}{M} \quad (2.13)$$

There is no formal recommendation about how to distribute the  $M$  angles into the sub-frequencies. One approach is to chose the angle randomly for each frequency component, while another approach is to assign a wave angle into each frequency with an ascending order as followings

$$\theta_n = \theta_{min} + n' \Delta\theta \quad (2.14)$$

where,  $n' = (n - 1) \bmod M$ . The length of synthesized waves from this method is  $T'_{max} = M \cdot T_{max}$ , although only  $T_{max}$  is requested for the time domain analysis.

Although the frequency spacing is clearly artificial, the wave field should become realistic for sufficiently large  $M$  and sufficiently small  $\Delta\omega$ . Based on the cross-spectrum analysis, Mile and Funke[8] found that minimum number of 32 wave directions should be used to guarantee the reasonable accuracy.

## 2.3 Equal Energy Method

This method to simulate directional waves assigns each frequency component of the wave to one of  $M$  discrete wave directions and a commercial code OrcaFlex uses this method to simulate a wave time history. Unlike the single summation method, the equal energy method does not divide each frequency band  $\Delta\omega$  into  $M$  sub-frequencies. Each wave direction will have the same number of frequencies assigned to it. In order to preserve the energy distribution in the wave spreading function, the wave directions are assigned so that a greater number of directions are concentrated near the central frequency. The wave elevation evaluated by the equal energy method is given by

$$\eta(\vec{x}, t) = Re \left[ \sum_{n=1}^N A_n \exp(i\omega_n t - i|\vec{k}_n|(x \cos \theta_n + y \sin \theta_n)) \right] \quad (2.15)$$

The complex amplitudes,  $A_n$  are given by

$$A_n = \underbrace{[\sqrt{2S(\omega_n)\Delta\omega}]_{a_n}} \exp(i\varepsilon_n) \quad (2.16)$$

### 2.3.1 Frequency Independent spreading function, $D(\theta)$

This method is only valid if the directional spreading function  $D(\omega, \theta)$  is independent in frequency component as follows:

$$S(\omega, \theta) = S(\omega)D(\theta) \quad (2.17)$$

There are several ways to define the directional spreading function. The most commonly used is *COSINE* –  $2s$  spreading function, which was proposed by Longuet-Higgins et al. [3] and given by

$$D(\theta) = C \left| \cos \left( \frac{\pi(\theta - \bar{\theta})}{\delta\theta} \right) \right|^{2s}, \quad (2.18)$$

where,  $S$  is the spreading parameter and the normalization constant,  $C$ , is given by

$$C = \frac{\sqrt{\pi}\Gamma(s+1)}{\delta\theta\Gamma(s+1/2)}, \quad (2.19)$$

and  $\Gamma$  is the gamma function. The cumulative energy distribution within the wave spreading function up to angle  $\theta$  is given by

$$P(\theta) = \int_{\bar{\theta} - \delta\theta/2}^{\theta} D(\theta') d\theta'. \quad (2.20)$$

where,  $\bar{\theta}$  is a mean wave direction.

The following method may be used to set the appropriate wave directions to satisfy the equal energy approach.

- Step1: Discretize the wave direction range  $\delta\theta$  by  $n_d$  steps and calculate  $D(\theta)$  spreading function. Set  $n_d$  to a sufficiently large number such that the function is smooth enough for interpolation over  $M$  directions (set  $n_d = 3M$ ).

- Step2: While calculating  $D(\theta)$ , calculate the cumulative energy sum up to the current direction as  $P(\theta)$ .
- Step3: Discretize  $P(\theta)$  into  $M$  steps from  $1/M \leq P_i \leq 1 - 1/M$ . Interpolate the function  $D(\theta)$  found in step 1 to find the corresponding values of  $\theta_i$ . The  $\theta_i$  values are the wave directions used in the equal energy method.
- Step4: Randomly assign each of the  $N$  frequencies (ignoring the end frequencies at which the wave amplitude is defined as zero) to a  $\theta_i$  direction such that each wave direction has  $N/M$  frequencies assigned to it.

### 2.3.2 Frequency dependent spreading function, $D(\omega, \theta)$

In many cases, for simplicity, it is assumed that the directional spreading function is independent of frequency. However, if someone need to simulate wave time series based on directional wave spectrum with frequency dependent spreading function such as a directional spectra measured by a buoy, the procedure presented in sec.2.3.1 is invalid. Especially, when both wave energy from swell system and local wind sea are significant, the assumption that the directional spreading function is independent of frequency is unreasonable because the mean wave direction and the degree of directional spreading of two ocean systems may be significantly different; generally, a spreading parameter  $s$  corresponding to swell sea is larger than a spreading parameter corresponding to wind sea.

### 3 Second-order directional wave theory

The second-order directional wave theory proposed by Sharma and Dean [1] is an extension of the theory developed by Longuet-Higgins [3] for water of infinite depth to apply to water of arbitrary depth. The nonlinear boundary value problem is solved to the second order by a perturbation approach accounting for contributions from linear components from arbitrary frequencies and directions. The second-order wave system is one that is forced by the linear system and all information on second-order amplitudes and phases are related to the characteristics of the first-order spectrum.

#### 3.1 Boundary value problem formulations

If the effects of viscosity and turbulence can be regarded as small, incompressible flows can be described well by a velocity potential. In other words, the velocity components  $u$ ,  $v$ , and  $w$  can be defined in terms of the gradients of the velocity potential  $\phi$  in the three Cartesian directions,  $x$ ,  $y$ , and  $z$ .

$$(u, v, w) = \left( \frac{\partial \phi}{\partial x}, \frac{\partial \phi}{\partial y}, \frac{\partial \phi}{\partial z} \right) \quad (3.1)$$

The mass conservation equation for an incompressible fluid is

$$\frac{\partial u}{\partial x} + \frac{\partial v}{\partial y} + \frac{\partial w}{\partial z} = 0 \quad (3.2)$$

which can be combined with Eq. 3.1 to yield

$$\nabla^2 \phi = \frac{\partial^2 \phi}{\partial x^2} + \frac{\partial^2 \phi}{\partial y^2} + \frac{\partial^2 \phi}{\partial z^2} = 0 \quad (3.3)$$

where,  $-h \leq z \leq \eta$  and  $-\infty \leq x, y \leq \infty$

Sharma and Dean proposed a second-order velocity potential function which satisfies the appropriate boundary conditions for the problem.

##### 3.1.1 Bottom Boundary Condition(BBC)

At the bottom boundary, the velocity normal to the boundary is equal to zero. For this case of a horizontal boundary at depth  $h$ ,

$$\frac{\partial \phi}{\partial z} \Big|_{z=-h} = 0 \quad (3.4)$$

##### 3.1.2 Kinematics Free Surface Boundary Condition(KFSBC)

A water particle on the free surface remains on the free surface and the vertical velocity at the free surface is equal to the total rate of change of water elevation.

$$\frac{\partial \eta}{\partial t} + \frac{\partial \phi}{\partial x} \frac{\partial \eta}{\partial x} + \frac{\partial \phi}{\partial y} \frac{\partial \eta}{\partial y} = \frac{\partial \phi}{\partial z} \quad (3.5)$$

where,  $z = \eta$

### 3.1.3 Dynamic Free Surface Boundary Conditions(DFSBC)

The pressure  $p$  follows from Bernoulli's equation and we can write as follows:

$$\frac{p}{\rho} + gz + \frac{\partial \phi}{\partial t} + \frac{1}{2} \nabla \phi \cdot \nabla \phi = -Q(t) \quad (3.6)$$

where,  $Q(t)$  is defined as an arbitrary function of time. Here, instead of including the time dependence of  $Q$  in the velocity potential  $\phi$ , let  $Q$  be a constant. At the free surface  $z = \eta$ , the pressure is equal to the atmospheric pressure,  $p_{atm}$  and if we choose  $Q = -p_{atm}/\rho$  in Eq.3.6 we can rewrite the equation as [9]

$$\Rightarrow g\eta + \frac{\partial \phi}{\partial t} + \frac{1}{2} \nabla \phi \cdot \nabla \phi = 0 \quad (3.7)$$

### 3.1.4 Combined Free Surface Boundary Condition(CFSBC)

This is an alternative form of Eqs.3.5 and 3.7 above in which, by eliminating the unknown free surface elevation  $\eta$ , involves only  $\phi$  and its derivatives.

$$-\frac{\partial^2 \phi}{\partial t^2} - g \frac{\partial \phi}{\partial z} - \left( \frac{\partial}{\partial t} + \frac{1}{2} \nabla \phi \cdot \nabla \right) |\nabla \phi|^2 = 0 \quad (3.8)$$

where,  $z = \eta$

## 3.2 Solution of the Boundary Value Problem

The perturbation approach is adopted for solution of the boundary value problem formulated in the previous section. This approach assumes that all variables can be expanded as a convergent power series of a small parameter, such as wave steepness. Also, it is assumed that the combined free surface boundary condition(CFSBC) can be expanded in a convergent Maclaurin series about the mean water level  $z = 0$  with a small parameter.

The velocity potential  $\phi$  and sea surface elevation  $\eta$  may be represented in the following manner with a perturbation parameter, wave steepness  $\varepsilon$ .

$$\phi(x, y, z, t) = \phi^{(1)}(x, y, z, t) + \phi^{(2)}(x, y, z, t) + \dots \quad (3.9)$$

$$\eta(x, y, t) = \eta^{(1)}(x, y, t) + \eta^{(2)}(x, y, t) + \dots \quad (3.10)$$

where,  $\eta^{(i)}$  and  $\phi^{(i)}$  is proportional to  $\varepsilon^i$  or  $O(\varepsilon^i)$ . By substituting the perturbation expansions for  $\phi$  and  $\eta$  into Laplace equation Eq.3.3 and the bottom boundary condition Eq.3.4, we can find two separated boundary conditions as follows:

$$\nabla^2 \phi^{(1)} = 0; \quad \nabla^2 \phi^{(2)} = 0 \quad (3.11)$$

$$\frac{\partial \phi^{(1)}}{\partial z} \Big|_{z=-h} = 0; \quad \frac{\partial \phi^{(2)}}{\partial z} \Big|_{z=-h} = 0 \quad (3.12)$$

Substituting the perturbation expansions into the dynamic free surface boundary condition(DFSBC) in Eq.3.7 and the combined free surface boundary condition(CFSBC)in Eq.3.8, we can separate terms of same orders ( $O(\varepsilon)$ ,  $O(\varepsilon^2)$ ,  $O(\varepsilon^3)$ , ...), just keep terms of  $O(\varepsilon)$  and  $O(\varepsilon^2)$ , and ignore terms of third or higher order ( $O(\varepsilon^3)$ ,  $O(\varepsilon^4)$ , ...); for example,  $\eta^{(1)}\phi^{(2)}$  and  $\eta^{(2)}\phi^{(1)}$  are the term of  $O(\varepsilon^3)$  and are ignored. From two boundary conditions, DFSBC and CFSBC, we obtain four additional equations as follows:

$$\frac{\partial^2 \phi^{(1)}}{\partial t^2} + g \frac{\partial \phi^{(1)}}{\partial z} = 0 \quad (3.13)$$

$$\frac{\partial^2 \phi^{(2)}}{\partial t^2} + g \frac{\partial \phi^{(2)}}{\partial z} = -\frac{\partial}{\partial t} |\nabla \phi^{(1)}|^2 - \eta^{(1)} \frac{\partial}{\partial t} \left[ \frac{\partial^2 \phi^{(1)}}{\partial t^2} + g \frac{\partial \phi^{(1)}}{\partial z} \right] \quad (3.14)$$

$$\eta^{(1)} = -\frac{1}{g} \frac{\partial \phi^{(1)}}{\partial t} \quad (3.15)$$

$$\eta^{(2)} = -\frac{1}{g} \left( \frac{\partial \phi^{(2)}}{\partial t} + \frac{1}{2} |\nabla \phi^{(1)}|^2 \right) - \frac{1}{g} \eta^{(1)} \frac{\partial^2 \phi^{(1)}}{\partial z \partial t} \quad (3.16)$$

where,  $z = 0$

### 3.2.1 First-Order Solution

First, we can select a first-order velocity potential,  $\phi^{(1)}$  of the following form

$$\phi^{(1)}(\vec{x}, z, t) = (-1) \cdot \sum_{n=1}^N \frac{g}{\omega_n} a_n \frac{\cosh[|\vec{k}_n|(h+z)]}{\cosh(|\vec{k}_n|h)} \sin(\omega_n t - \vec{k}_n \cdot \vec{x} + \varepsilon_n) \quad (3.17)$$

$$\Rightarrow \phi^{(1)}(\vec{x}, z, t) = \text{Re} \left[ \sum_{n=1}^N i \frac{g}{\omega_n} A_n \frac{\cosh[|\vec{k}_n|(h+z)]}{\cosh(|\vec{k}_n|h)} \exp(i\omega_n t - i\vec{k}_n \cdot \vec{x}) \right] \quad (3.18)$$

which satisfies Eq.3.11, 3.12, and 3.13. By substituting Eq.3.17 into Eq.3.15, we obtain the first-order components of the surface wave elevation,  $\eta^{(1)}$

$$\eta^{(1)}(\vec{x}, t) = \sum_{n=1}^N a_n \cos(\omega_n t - \vec{k}_n \cdot \vec{x} + \varepsilon_n) \quad (3.19)$$

$$\Rightarrow \eta^{(1)}(\vec{x}, t) = \text{Re} \left[ \sum_{n=1}^N A_n \exp(i\omega_n t - i\vec{k}_n \cdot \vec{x}) \right] \quad (3.20)$$

where,  $A_n = a_n \exp(i\varepsilon_n)$ ;  $\vec{x} = (x, y)$  is a point on the horizontal  $x$ - $y$  plane;  $\omega_n$  is the angular frequency;  $\vec{k}_n$  is the wave number which is related to the frequency,  $\omega_n$ , through the linear dispersion relation,  $\omega_n^2 = g|\vec{k}_n| \tanh(|\vec{k}_n|h)$  (where  $h$  is the water depth);  $N$  is the total number of frequencies considered. Also,  $a_n$  are the component spectral amplitudes, which are calculated as follows:

$$E \left[ \frac{a_n^2}{2} \right] = S(\omega_n) \Delta \omega \quad (3.21)$$

where,  $E[\bullet]$  is the expected value of  $\bullet$ .

### 3.2.2 Second-Order Solution

Second-order waves are obtained as a result of the sum and difference interactions between pairs of frequencies and the phases of the second-order contributions are determined by the sum and difference interactions of the phases of the first-order component phases, which are random. The second-order velocity potential which satisfies Eq.3.11, 3.12, and 3.14 is given as follows:

$$\phi^{(2)}(\vec{x}, z, t) = (-1) \cdot \sum_{n=1}^N \sum_{m=1}^N a_n a_m \cdot B_{nm}^{\pm} \cdot \sin \left( (\omega_n \pm \omega_m)t - (\vec{k}_n \pm \vec{k}_m) \cdot \vec{x} + (\varepsilon_n \pm \varepsilon_m) \right) \quad (3.22)$$

$$\Rightarrow \phi^{(2)}(\vec{x}, z, t) = Re \left[ \sum_{n=1}^N \sum_{m=1}^N i A_n A_m \cdot B_{nm}^{\pm} \cdot \exp \left( i(\omega_n \pm \omega_m)t - i(\vec{k}_n \pm \vec{k}_m) \cdot \vec{x} \right) \right] \quad (3.23)$$

By substituting for the first-order potential  $\phi^{(1)}$ , the first-order surface elevation  $\eta^{(1)}$ , and the second-order potential  $\phi^{(2)}$  in Eq.3.16, we obtain the second-order correction to the linear sea surface elevation as follows:

$$\eta^{(2)}(\vec{x}, t) = \sum_{n=1}^N \sum_{m=1}^N a_n a_m \cdot L_{nm}^{\pm} \cdot \cos \left( (\omega_n \pm \omega_m)t - (\vec{k}_n \pm \vec{k}_m) \cdot \vec{x} + (\varepsilon_n \pm \varepsilon_m) \right) \quad (3.24)$$

$$\Rightarrow \eta^{(2)}(\vec{x}, t) = Re \left[ \sum_{n=1}^N \sum_{m=1}^N A_n A_m \cdot L_{nm}^{\pm} \cdot \exp \left( i(\omega_n \pm \omega_m)t - i(\vec{k}_n \pm \vec{k}_m) \cdot \vec{x} \right) \right] \quad (3.25)$$

The transfer function derived by Sharma and Dean,  $L_{nm}^{\pm}$  and  $B_{nm}^{\pm}$  are given by:

$$L_{nm}^{\pm}(\omega_n, \omega_m, \theta_n, \theta_m) = \frac{1}{4} \left[ \frac{D_{nm}^{\pm} - (|\vec{k}_n| |\vec{k}_m| \cos(\theta_n - \theta_m) \mp R_n R_m)}{\sqrt{R_n R_m}} + (R_n + R_m) \right] \quad (3.26)$$



$$B_{nm}^{\pm}(z, \omega_n, \omega_m, \theta_n, \theta_m) = \frac{g^2}{\omega_n \omega_m} \cdot \frac{1}{4} \frac{\cosh[k_{nm}^{\pm}(h+z)]}{\cosh[k_{nm}^{\pm}(h)]} \frac{D_{nm}^{\pm}}{\omega_n \pm \omega_m} \quad (3.27)$$

where,

$$R_n = |\vec{k}_n| \tanh(|\vec{k}_n| h) \quad (3.28)$$



$$D_{nm}^{\pm} = \frac{\{(\sqrt{R_n} \pm \sqrt{R_m})[\sqrt{R_m}(k_n^2 - R_n^2) \pm \sqrt{R_n}(k_m^2 - R_m^2)]\}}{[(\sqrt{R_n} \pm \sqrt{R_m})^2 - k_{nm}^{\pm} \tanh(k_{nm}^{\pm} h)]} + \frac{[2(\sqrt{R_n} \pm \sqrt{R_m})^2][|\vec{k}_n| |\vec{k}_m| \cos(\theta_n - \theta_m) \mp R_n R_m]}{[(\sqrt{R_n} \pm \sqrt{R_m})^2 - k_{nm}^{\pm} \tanh(k_{nm}^{\pm} h)]} \quad (3.29)$$

In the above,  $k_{nm}^+$  and  $k_{nm}^-$  are given as follows :

$$\begin{aligned} k_{nm}^+ &= \sqrt{k_n^2 + k_m^2 + 2k_n k_m \cos(\theta_n - \theta_m)} \\ k_{nm}^- &= \sqrt{k_n^2 + k_m^2 - 2k_n k_m \cos(\theta_n - \theta_m)} \end{aligned} \quad (3.30)$$

For infinite depth, the equations proposed by Sharma and Dean [1] reduces to the equations derived by Longuet-Higgins et al. [3] for deep water. Also, for  $\vec{k}_n = \vec{k}_m$  and  $N = 1$ , the formulas for velocity potential and surface elevation reduce to the familiar Stokes second-order equations [2].

### 3.3 Validity of the Second-order Wave theory

While the second-order irregular wave model is a more accurate representation of irregular seas in shallow waters compared to the linear irregular wave model, it obviously does not model the complete nonlinear character of waves, and is not valid for all cases. The physical parameter that determines the range of validity is the wave steepness. When the wave steepness exceeds a certain value, the second-order model is no longer valid, and a higher-order model is required. In fact, when waves become too steep, they can break and no model based on solution of Laplace's equation (in terms of velocity potential) is valid.

## 4 Second-Order Wave Kinematics

It is assumed that the considered fluid is incompressible, inviscid, and irrotational. Specially, the velocity fields of irrotational fluid can be expressed as follows:

$$\vec{u} = \nabla\phi \quad (4.1)$$

$$\vec{u}^{(1)} = (u_x^{(1)}, u_y^{(1)}, u_z^{(1)}) = \nabla\phi^{(1)} = \left( \frac{\partial\phi^{(1)}}{\partial x}, \frac{\partial\phi^{(1)}}{\partial y}, \frac{\partial\phi^{(1)}}{\partial z} \right) \quad (4.2)$$

$$\vec{u}^{(2)} = (u_x^{(2)}, u_y^{(2)}, u_z^{(2)}) = \nabla\phi^{(2)} = \left( \frac{\partial\phi^{(2)}}{\partial x}, \frac{\partial\phi^{(2)}}{\partial y}, \frac{\partial\phi^{(2)}}{\partial z} \right) \quad (4.3)$$

The acceleration of a water particle can be evaluated by the material or substantial derivative of velocity vector,  $\vec{u}$ .

$$\frac{D}{Dt}\vec{u} = \underbrace{\frac{\partial\vec{u}}{\partial t}}_{Term1} + \underbrace{\vec{u} \cdot \nabla\vec{u}}_{Term2} \quad (4.4)$$

where, *Term1* and *Term2* are called the local acceleration at a fixed point and the convective acceleration, respectively. However, we are only interested in the acceleration a fixed point, which is evaluated as follows:

$$\vec{a}^{(1)} = (a_x^{(1)}, a_y^{(1)}, a_z^{(1)}) = \frac{\partial\vec{u}^{(1)}}{\partial t} = \left( \frac{\partial u_x^{(1)}}{\partial t}, \frac{\partial u_y^{(1)}}{\partial t}, \frac{\partial u_z^{(1)}}{\partial t} \right) \quad (4.5)$$

$$\vec{a}^{(2)} = (a_x^{(2)}, a_y^{(2)}, a_z^{(2)}) = \frac{\partial\vec{u}^{(2)}}{\partial t} = \left( \frac{\partial u_x^{(2)}}{\partial t}, \frac{\partial u_y^{(2)}}{\partial t}, \frac{\partial u_z^{(2)}}{\partial t} \right) \quad (4.6)$$

To obtain the first- and second-order pressure, let substitute the perturbation expansions of velocity potential into the Bernoulli's equation in Eq.3.6 and separate terms of same order.

$$\frac{p}{\rho} + gz + \frac{\partial}{\partial t}(\phi^{(1)} + \phi^{(2)} + \dots) + \frac{1}{2}\nabla(\phi^{(1)} + \phi^{(2)} + \dots) \cdot \nabla(\phi^{(1)} + \phi^{(2)} + \dots) = -Q \quad (4.7)$$

$$\frac{p}{\rho} = -gz - Q + \underbrace{\left[ \frac{\partial\phi^{(1)}}{\partial t} \right]}_{O(\epsilon)} + \underbrace{\left[ \frac{\partial\phi^{(2)}}{\partial t} + \frac{1}{2}\nabla\phi^{(1)} \cdot \nabla\phi^{(1)} \right]}_{O(\epsilon^2)} + O(\epsilon^3) + \dots \quad (4.8)$$

Therefore, the first- and second-order dynamic pressure,  $p_d^{(1)}$  and  $p_d^{(2)}$  are obtained as follows [10] [11]:

$$p_d^{(1)} = -\rho \frac{\partial\phi^{(1)}}{\partial t} \quad (4.9)$$

$$p_d^{(2)} = -\rho \left[ \frac{\partial \phi^{(2)}}{\partial t} + \frac{1}{2} \nabla \phi^{(1)} \cdot \nabla \phi^{(1)} \right] = \underbrace{-\rho \left[ \frac{\partial \phi^{(2)}}{\partial t} \right]}_{Term1} \underbrace{-\rho \left[ \frac{1}{2} \vec{u}^{(1)} \cdot \vec{u}^{(1)} \right]}_{Term2} \quad (4.10)$$

where, *Term1* and *Term2* are called the second-order potential term and quadratic interaction term, respectively.

## 4.1 Wave Surface Elevation

$$\eta^{(1)}(\vec{x}, t) = Re \left[ \sum_{n=1}^N A_n \exp(-i\vec{k}_n \cdot \vec{x}) \exp(i\omega_n t) \right] \quad (4.11)$$

$$\eta^{(2\pm)}(\vec{x}, t) = Re \left[ \sum_{n=1}^N \sum_{m=1}^N A_{nm}^{\pm} K_{nm}^{\pm} \cdot \exp(-i(\vec{k}_n \pm \vec{k}_m) \cdot \vec{x}) \exp(i\omega_{nm}^{\pm} t) \right] \quad (4.12)$$

where,

$$\varepsilon_{nm}^{\pm} = \varepsilon_n \pm \varepsilon_m \quad \text{and} \quad \omega_{nm}^{\pm} = \omega_n \pm \omega_m \quad (4.13)$$

$$K_{nm}^{\pm} = L_{nm}^{\pm} \quad (4.14)$$

$$A_{nm}^+ = A_n A_m \quad \text{and} \quad A_{nm}^- = A_n A_m^* \quad (4.15)$$

## 4.2 Wave Particle Velocity

### 4.2.1 First-Order

$$u_x^{(1)}(\vec{x}, z, t) = Re \left[ \sum_{n=1}^N A_n \omega_n \frac{\cosh[|\vec{k}_n|(h+z)]}{\sinh(|\vec{k}_n|h)} \cos \theta_n \exp(-i\vec{k}_n \cdot \vec{x}) \exp(i\omega_n t) \right] \quad (4.16)$$

$$u_y^{(1)}(\vec{x}, z, t) = Re \left[ \sum_{n=1}^N A_n \omega_n \frac{\cosh[|\vec{k}_n|(h+z)]}{\sinh(|\vec{k}_n|h)} \sin \theta_n \exp(-i\vec{k}_n \cdot \vec{x}) \exp(i\omega_n t) \right] \quad (4.17)$$

$$u_z^{(1)}(\vec{x}, z, t) = Re \left[ (i) \cdot \sum_{n=1}^N A_n \omega_n \frac{\sinh[|\vec{k}_n|(h+z)]}{\sinh(|\vec{k}_n|h)} \exp(-i\vec{k}_n \cdot \vec{x}) \exp(i\omega_n t) \right] \quad (4.18)$$

### 4.2.2 Second-Order



$$u_x^{(2\pm)}(\vec{x}, z, t) = Re \left[ \sum_{n=1}^N \sum_{m=1}^N A_{nm}^{\pm} \cdot x \dot{U}_{nm}^{\pm} \cdot \exp(-i(\vec{k}_n \pm \vec{k}_m) \cdot \vec{x}) \cdot \exp(i\omega_{nm}^{\pm} t) \right] \quad (4.19)$$

$$u_y^{(2\pm)}(\vec{x}, z, t) = Re \left[ \sum_{n=1}^N \sum_{m=1}^N A_{nm}^{\pm} \cdot y \dot{U}_{nm}^{\pm} \cdot \exp(-i(\vec{k}_n \pm \vec{k}_m) \cdot \vec{x}) \cdot \exp(i\omega_{nm}^{\pm} t) \right] \quad (4.20)$$

$$u_z^{(2\pm)}(\vec{x}, z, t) = \text{Re} \left[ \sum_{n=1}^N \sum_{m=1}^N A_{nm}^{\pm} \cdot z \dot{U}_{nm}^{\pm} \cdot \exp(-i(\vec{k}_n \pm \vec{k}_m) \cdot \vec{x}) \cdot \exp(i\omega_{nm}^{\pm} t) \right] \quad (4.21)$$

where,

$${}_x U_{nm}^{\pm} = B_{nm}^{\pm} \cdot (|\vec{k}_n| \cos \theta_n \pm |\vec{k}_m| \cos \theta_m) \quad (4.22)$$

$${}_y U_{nm}^{\pm} = B_{nm}^{\pm} \cdot (|\vec{k}_n| \sin \theta_n \pm |\vec{k}_m| \sin \theta_m) \quad (4.23)$$

$${}_z U_{nm}^{\pm} = (i) \cdot B_{nm}^{\pm} \cdot k_{nm}^{\pm} \cdot \tanh[k_{nm}^{\pm}(h+z)] \quad (4.24)$$

### 4.3 Wave Particle Acceleration

#### 4.3.1 First-Order

$$a_x^{(1)}(\vec{x}, z, t) = \text{Re} \left[ (i) \cdot \sum_{n=1}^N A_n \omega^2 \frac{\cosh[|\vec{k}_n|(h+z)]}{\sinh(|\vec{k}_n|h)} \cos \theta_n \exp(-i\vec{k}_n \cdot \vec{x}) \exp(i\omega_n t) \right] \quad (4.25)$$

$$a_y^{(1)}(\vec{x}, z, t) = \text{Re} \left[ (i) \cdot \sum_{n=1}^N A_n \omega^2 \frac{\cosh[|\vec{k}_n|(h+z)]}{\sinh(|\vec{k}_n|h)} \sin \theta_n \exp(-i\vec{k}_n \cdot \vec{x}) \exp(i\omega_n t) \right] \quad (4.26)$$

$$a_z^{(1)}(\vec{x}, z, t) = \text{Re} \left[ \sum_{n=1}^N A_n (-1) \omega^2 \frac{\sinh[|\vec{k}_n|(h+z)]}{\sinh(|\vec{k}_n|h)} \exp(-i\vec{k}_n \cdot \vec{x}) \exp(i\omega_n t) \right] \quad (4.27)$$

#### 4.3.2 Second-Order

$$a_x^{(2\pm)}(\vec{x}, z, t) = \text{Re} \left[ \sum_{n=1}^N \sum_{m=1}^N A_{nm}^{\pm} \cdot {}_x \dot{U}_{nm}^{\pm} \cdot \exp(-i(\vec{k}_n \pm \vec{k}_m) \cdot \vec{x}) \cdot \exp(i\omega_{nm}^{\pm} t) \right] \quad (4.28)$$

$$a_y^{(2\pm)}(\vec{x}, z, t) = \text{Re} \left[ \sum_{n=1}^N \sum_{m=1}^N A_{nm}^{\pm} \cdot {}_y \dot{U}_{nm}^{\pm} \cdot \exp(-i(\vec{k}_n \pm \vec{k}_m) \cdot \vec{x}) \cdot \exp(i\omega_{nm}^{\pm} t) \right] \quad (4.29)$$

$$a_z^{(2\pm)}(\vec{x}, z, t) = \text{Re} \left[ \sum_{n=1}^N \sum_{m=1}^N A_{nm}^{\pm} \cdot {}_z \dot{U}_{nm}^{\pm} \cdot \exp(-i(\vec{k}_n \pm \vec{k}_m) \cdot \vec{x}) \cdot \exp(i\omega_{nm}^{\pm} t) \right] \quad (4.30)$$

where,

$${}_x \dot{U}_{nm}^{\pm} = (i) \cdot {}_x U_{nm}^{\pm} \cdot \omega_{nm}^{\pm} \quad (4.31)$$

$${}_y \dot{U}_{nm}^{\pm} = (i) \cdot {}_y U_{nm}^{\pm} \cdot \omega_{nm}^{\pm} \quad (4.32)$$

$${}_z \dot{U}_{nm}^{\pm} = (i) {}_z U_{nm}^{\pm} \cdot \omega_{nm}^{\pm} \quad (4.33)$$

## 4.4 Dynamic Pressure

### 4.4.1 First-Order

$$p^{(1)}(\vec{x}, z, t) = \text{Re} \left[ \sum_{n=1}^N A_n \rho_w g \frac{\cosh[|\vec{k}_n|(h+z)]}{\cosh(|\vec{k}_n|h)} \exp(-i\vec{k}_n \cdot \vec{x}) \exp(i\omega_n t) \right] \quad (4.34)$$

### 4.4.2 Second-Order (only second-order potential term)

$$p^{(2\pm)}(\vec{x}, z, t) = \text{Re} \left[ \sum_{n=1}^N \sum_{m=1}^N A_{nm}^{\pm} \cdot P_{nm}^{\pm} \cdot \exp(-i(\vec{k}_n \pm \vec{k}_m) \cdot \vec{x}) \cdot \exp(i\omega_{nm}^{\pm} t) \right] \quad (4.35)$$

$$P_{nm}^{\pm} = \rho_w \cdot B_{nm}^{\pm} \cdot \omega_{nm}^{\pm} \quad (4.36)$$

## 4.5 Properties of Quadratic Transfer Function

### 4.5.1 Symmetricity of QTF

Similar expressions of the quadratic transfer function(QTF) arise in describing loads and responses of floating structure; in this case, the QTF are evaluated numerically from software tools for wave diffraction and radiation analysis such as WAMIT or AQWA. The QTFs ( $F_{mm}^{2\pm}$ ) used for evaluating second-order forces of a floating structure always have the following symmetry relations:

$$F^{2+}(\omega_n, \omega_m) = F^{2+}(\omega_m, \omega_n) \quad \text{and} \quad F^{2-}(\omega_n, \omega_m) = F^{2-}(\omega_m, \omega_n)^* \quad (4.37)$$

Symmetry relations in Eq.4.37 are also applicable to QTFs for second-order kinematics and this symmetricity property significantly reduce the computational effort by enabling to only take the lower- or upper-triangular part when someone numerically simulate wave kinematic.

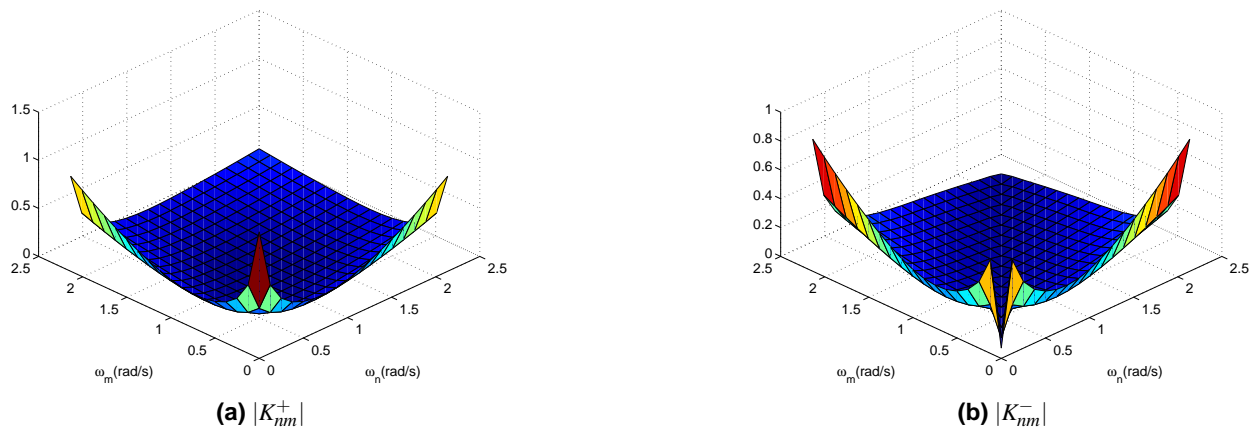


Figure 1. Transfer function for  $\eta^{2\pm}$  ( $\omega > 0$ ): unidirectional wave( $\theta_n = \theta_m = 0$ )

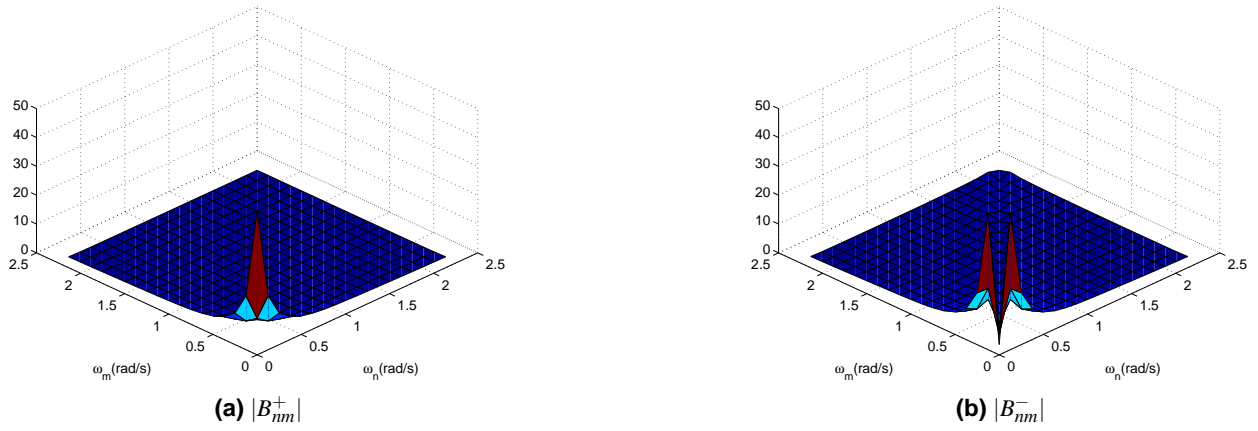


Figure 2. Transfer function for  $\phi^{2\pm}$  ( $\omega > 0$ ) at MSL( $h = 20m$ ): unidirectional wave( $\theta_n = \theta_m = 0$ )

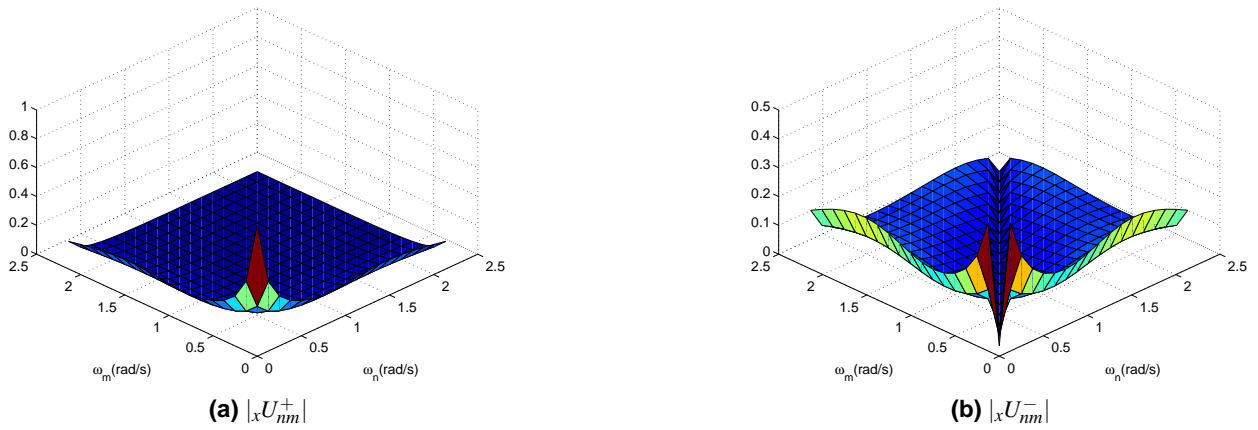


Figure 3. Transfer function for  $u_x^{2\pm}$  ( $\omega > 0$ ) at MSL( $h = 20m$ ): unidirectional wave( $\theta_n = \theta_m = 0$ )

#### 4.5.2 Singularity of QTF

Formulations for the first- and second-order wave kinematics shown in previous sections are determined from the solution of a boundary value problem(see Eq.3.3 - 3.8). When we implement the formulations to numerically simulate wave kinematics, these formulations have several restrictions, which stem from physically correct or weakly-correct assumptions considered during solving the boundary value problem. One of the restriction is the singularity of the first- and second-order wave kinematic transfer functions. The singularity problem is also shown in QTFs proposed by other researchers.(Longuet-Higgins [3]; Marthinsen and Winterstein [12]; Nwogu [13])

#### QTF proposed by Longuet-Higgins [3]

$$B_{nm}^{\pm} = \frac{g^2}{\omega_n \omega_m} \frac{(\omega_n \pm \omega_m)(\vec{k}_n \cdot \vec{k}_m \mp |\vec{k}_n||\vec{k}_m|)}{(\omega_n \pm \omega_m)^2 - g|\vec{k}_n \pm \vec{k}_m|} \quad (4.38)$$

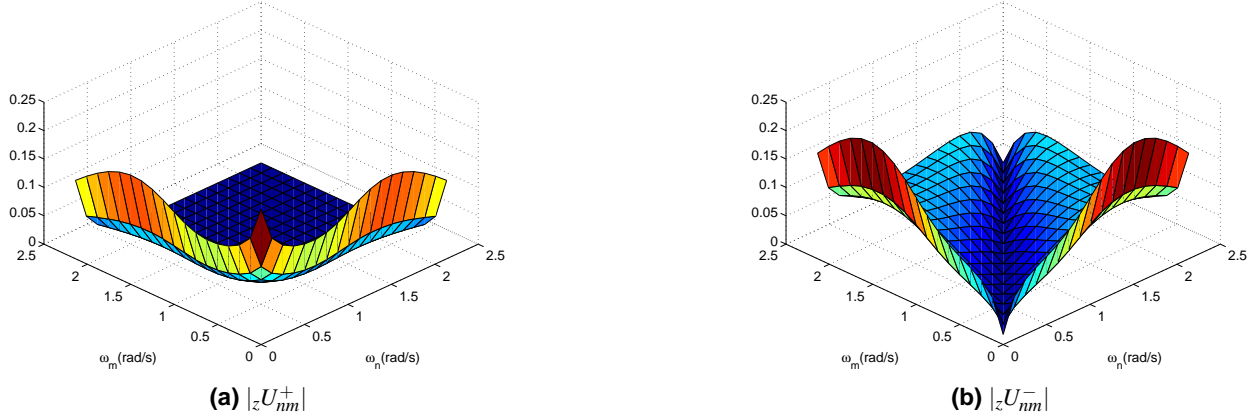


Figure 4. Transfer function for  $u_z^{\pm}$  ( $\omega > 0$ ) at MSL( $h = 20m$ ): unidirectional wave( $\theta_n = \theta_m = 0$ )

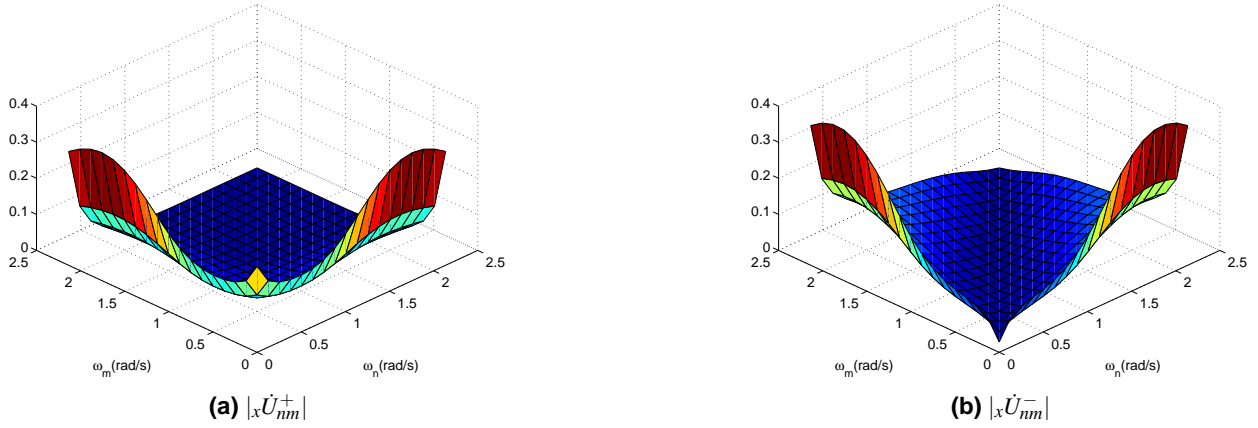


Figure 5. Transfer function for  $a_x^{\pm}$  ( $\omega > 0$ ) at MSL( $h = 20m$ ): unidirectional wave( $\theta_n = \theta_m = 0$ )

QTF used by Marthinsen and Winterstein [12]

$$B_{nm}^{\pm} = (1 - \delta_{-i,j}) \frac{g^2}{\omega_n \omega_m} \frac{\frac{g^2 |\vec{k}_n| |\vec{k}_m|}{2\omega_n \omega_m} - \frac{1}{4} (\omega_n^2 + \omega_m^2 \pm \omega_n \omega_m) + \frac{g^2}{4} \frac{\omega_n |\vec{k}_m|^2 \pm \omega_m |\vec{k}_n|^2}{\omega_n \omega_m (\omega_n \pm \omega_m)}}{(\omega_n \pm \omega_m) - g \frac{|\vec{k}_n| \pm |\vec{k}_m|}{\omega_n \pm \omega_m} \tanh[ (|\vec{k}_n| \pm |\vec{k}_m|) h ]} \quad (4.39)$$

where,  $\delta_{-i,j} = 1$  if  $n = m$ , zero otherwise and is introduced to avoid the singularity of  $B_{nm}^{\pm}$ .

QTF proposed by Nwogu [13]

$$K_{nm}^{\pm} = \frac{\omega_n \omega_m (k_{nm}^{\pm} h)^2 \cos(\theta_n - \theta_m) [1 - (\alpha + 1/3) (k_{nm}^{\pm} h)^2]}{2\lambda k'_n k'_m h^3} + \frac{\omega_{mn}^{\pm} [1 - \alpha (k_{nm}^{\pm} h)^2] [\omega_n k'_m h (|\vec{k}_n| h \pm |\vec{k}_m| h \cos(\theta_n - \theta_m)) + \omega_m k'_n h (|\vec{k}_n| h \cos(\theta_n - \theta_m) \pm |\vec{k}_m| h)]}{2\lambda k'_n k'_m h^3} \quad (4.40)$$

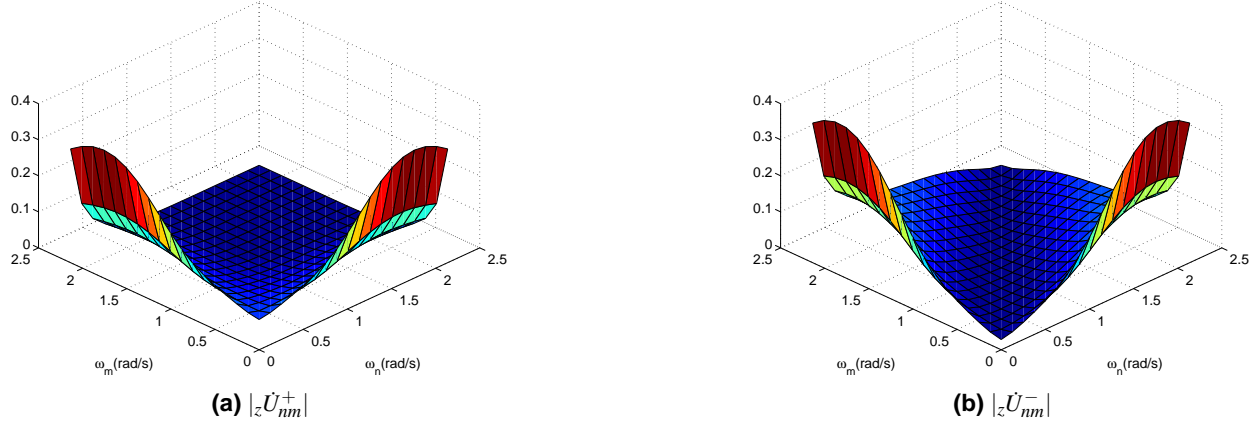


Figure 6. Transfer function for  $a_z^{\pm}$  ( $\omega > 0$ ) at MSL( $h = 20m$ ): unidirectional wave( $\theta_n = \theta_m = 0$ )

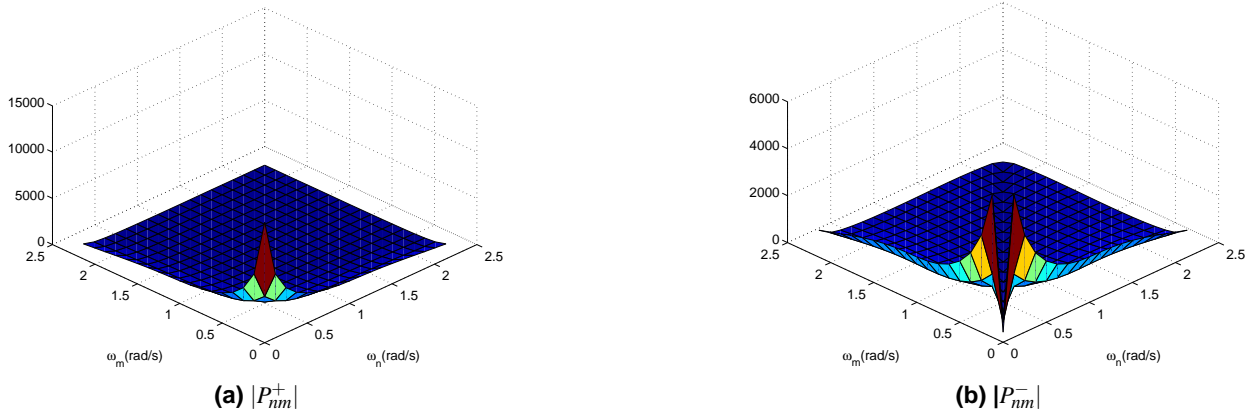


Figure 7. Transfer function for  $p^{2\pm}$  ( $\omega > 0$ ) at MSL( $h = 20m$ ): unidirectional wave( $\theta_n = \theta_m = 0$ )

$$\lambda = (\omega_{nm}^{\pm})^2 [1 - \alpha(k_{nm}^{\pm}h)^2] - g(k_{nm}^{\pm})^2 h [1 - (\alpha + 1/3)(k_{nm}^{\pm}h)^2] \quad (4.41)$$

$$k'_n = |\vec{k}_n| [1 - (\alpha + 1/3)(|\vec{k}_n|h)^2] \quad (4.42)$$

where,  $\alpha = (z_{\alpha}/h)^2/2 + (z_{\alpha}/h)$  and  $z_{\alpha} \approx -0.53h$  from shallow water depths up to the deep water depth limit.

### Singularity at $\omega = 0$

When  $\omega$  in Eq.3.17 approaches zero, the denominator of the equation approaches zero. Although the numerator also approaches zero, we may get an unwanted non-numerical value (so-called *NaN*), and a special treatment may be required during numerical simulation of the kinematics depending on what software tools are used. To avoid discontinuity or singularity problem at zero frequency, someone can simply set the kinematics equal to zero.

QTFs of the second-order wave elevation and velocity potential,  $L_{nm}^{\pm}$  and  $B_{nm}^{\pm}$  also have similar singularity issue at zero frequency. As shown in Eq.3.26, the denominator of the first term in  $L_{nm}^{\pm}$  is  $\sqrt{R_n R_m} = \sqrt{|\vec{k}_n| \tanh(|\vec{k}_n|h)} \sqrt{|\vec{k}_m| \tanh(|\vec{k}_m|h)}$ , which approaches zero when either  $\omega_n$  or  $\omega_m$  goes to zero.

One of the numerators of  $B_{nm}^{\pm}$  in Eq.3.27 is  $D_{nm}^{\pm}$  in Eq.3.29. The numerators of both first and second terms approaches zero when either  $\omega_n$  or  $\omega_m$  goes to zero. In this case, there is no need for any special treatment during a numerical simulation because the denominator of  $B_n^{\pm}m$  is not zero unless  $\omega_n = \omega_m = 0$ .

Based on the existence of singularity in the first- and second-order transfer functions, we presume that the formulations presented in sec.3.2 do not evaluate the first- and second-order wave kinematic when  $\omega_n = 0$  or  $\omega_m = 0$ . This presumption is physically understandable because we assume that the a zero frequency regular wave does not have any wave energy and the zero-energy wave component does not enable to interact with any other wave components. Please refer to Fig.8 and 9 to check the singularity issue at  $\omega = 0$ .

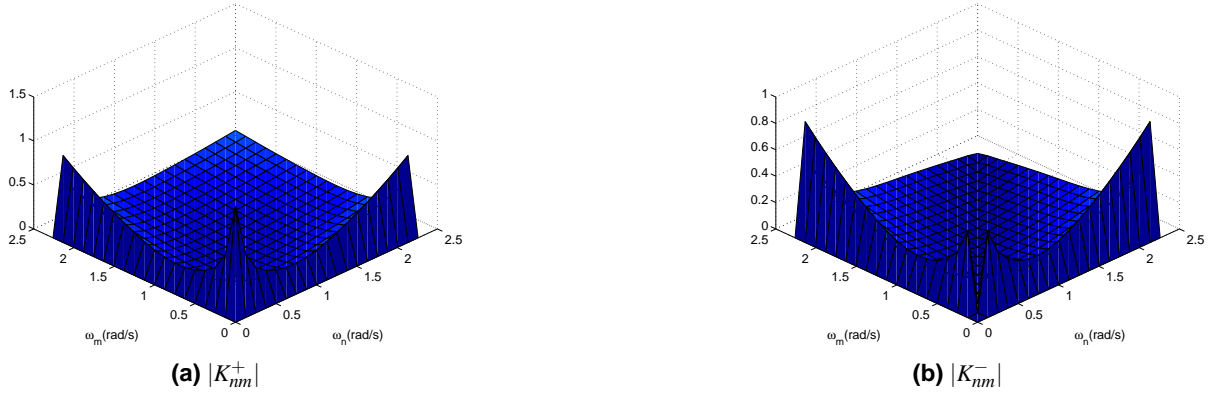


Figure 8. Transfer function  $K_{nm}^{\pm}$  including  $\omega = 0$

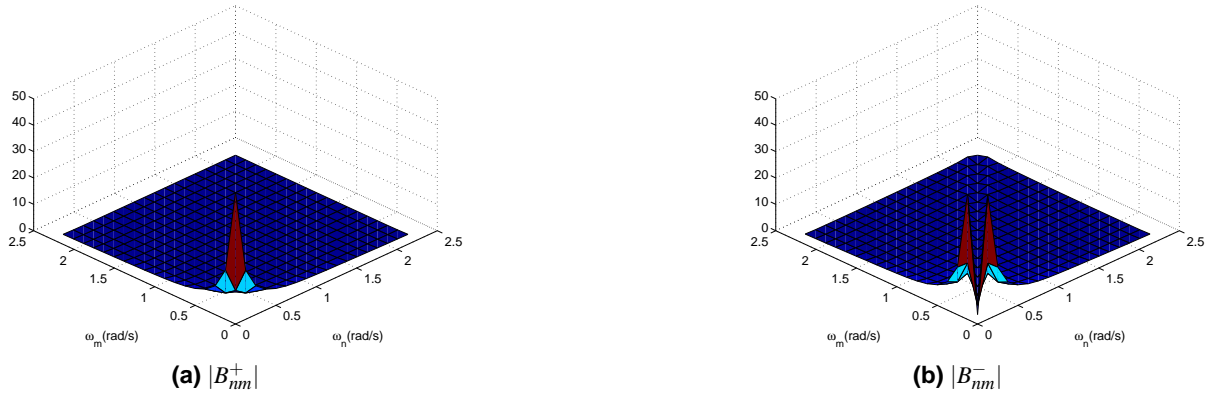


Figure 9. Transfer function  $B_{nm}^{\pm}$  including  $\omega = 0$

### Singularity at diagonal components of $L_{nm}^-$ and $B_{nm}^-$

Another singularity considered during numerical simulation is the discontinuity in diagonal component of  $L_{nm}^-$  and  $B_{nm}^-$ . When  $\omega_n = \omega_m$ , the denominator terms of  $D_{nm}^-$  equal to zero, which makes  $L_{nm}^-$  and  $B_{nm}^-$  singular along the diagonal components. Physically, the interaction between two wave components propagating to opposite direction with same magnitude results in total energy loss. It can be explained through Fig.10, which shows how to interact

two wave components. As shown in Fig.10, two free wave component  $\vec{k}_n$  and  $\vec{k}_m$  generates new bounded wave components  $\vec{k}_n + \vec{k}_m$  and  $\vec{k}_n - \vec{k}_m$  by summation interaction and difference interaction, respectively.

Therefore, unlike difference interaction QTFs for second order wave force, all diagonal components of  $L_{nm}^-$  and  $B_{nm}^-$  should be set to zero, which means total energy loss by the interaction between two wave components with same magnitude and difference propagation direction,  $\vec{k}_n - \vec{k}_n$ . This is apparent for the QTF of velocity potential,  $B_{nm}^-$  because the sign of upper triangular part in  $B_{nm}^-$  is opposite to the lower triangular part.

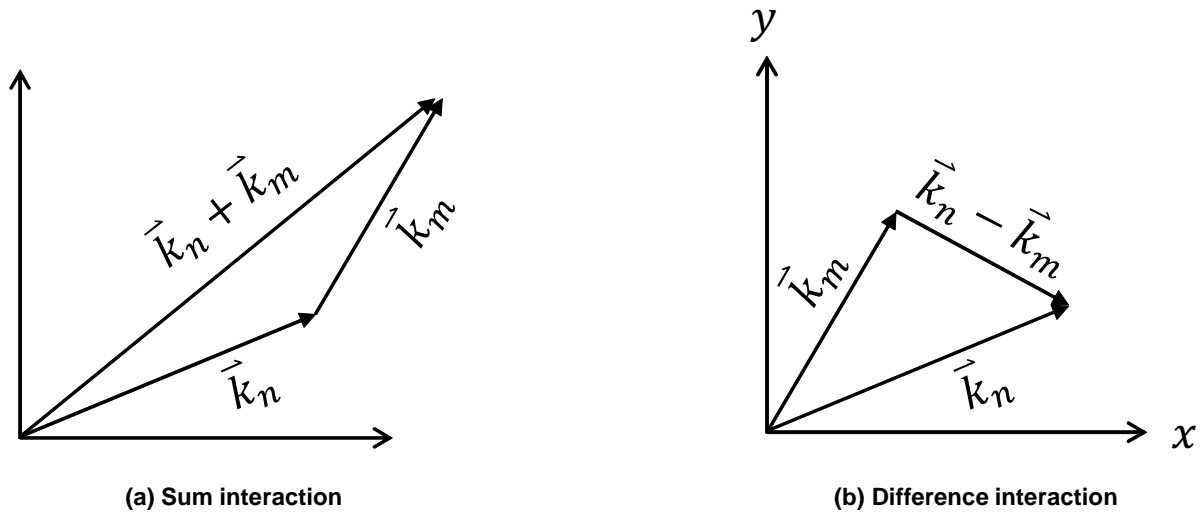


Figure 10. The sum and difference interaction of the wavenumber vectors



## 5 Numerical Simulation of Second-Order Wave Kinematics

In this chapter, the equations and algorithms used to numerically evaluating the second order wave kinematics based on the linear or first order wave properties. The forms of the equations presented here are what is used in the Wave2 module within HydroDyn. Before presenting the equations, we first discuss the validity issue of the second order wave theory briefly introduced in sec.3.3.

### 5.1 Limitation of Second-Order Wave Theory

As shown in sec.3.2, the solutions of the second-order boundary value problem are derived based on a perturbation approach, which uses a wave steepness,  $\varepsilon \ll 1$  as an expansion parameter. For a regular wave component, Dean and Dalrymple defined  $\varepsilon = ka/2$ , where  $k$  and  $a$  are wavenumber and wave amplitude. According to Dean and Dalrymple, the second-order wave theory is valid if two criteria are fulfilled as follows:

- **Convergence:** First, the ratio of the second-order term to the first order term in Eq.3.9 must be much smaller than 1.

$$\frac{\varepsilon^2 \phi^{(2)}}{\varepsilon \phi^{(1)}} = \frac{ka\phi^{(2)}}{2\phi^{(1)}} \ll 1 \quad (5.1)$$

$$\Rightarrow \frac{3}{8} \frac{ka \cosh(2kh)}{\cosh(kh) \sinh^3(kh)} \ll 1 \quad (5.2)$$

- **No bump in the trough:** Second, the physical properties of the wave profile require that there is no bump in the trough. This is indicated by a negative second derivative of the wave trough, which lead to the criterion

$$ka < \frac{\sinh^3(kh)}{\cosh(kh)[2 + \cosh(2kh)]} \quad (5.3)$$

In addition to the above two criteria, the breaking criterion for the wave steepness must be fulfilled. One of the breaking wave criteria in arbitrary water depth is given by the Miche breaking criterion

$$\frac{H}{L} = \frac{2a}{2\pi/k} < 0.142 \tanh(kh) \quad (5.4)$$

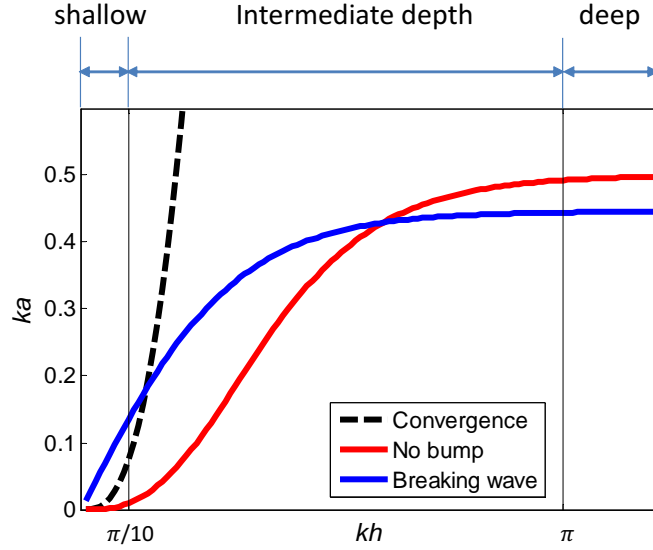
$$\Rightarrow ka < 0.142\pi \tanh(kh) \quad (5.5)$$

Fig.11 illustrates the different criteria of  $ka$  as a function of  $kh$ . Except when  $kh \rightarrow 0$ , the convergence criteria is satisfied when the criterion for no bump in the trough and wave breaking criterion are satisfied. When  $kh > 0.62\pi$ , the maximum wave steepness is restricted by the breaking wave criterion.

In a regular wave case, the validity of second-order wave theory can be simply controlled by limiting the considered maximum wavenumber to satisfy the three criteria(see Eq.5.2, 5.3, and 5.5). However, because these criteria were derived for a regular wave case, it may or may not be physically correct to directly expand the criteria to the irregular wave case. The following three criteria can be used to evaluate the maximum wave frequency for the valid application of the second-order wave theory.

- **Hu and Zhao [14]:** Based on results from numerical simulations, Hu and Zhao suggested that the second-order wave model presented here is valid as long as  $H_s/L_z$  is smaller than approximately 0.08, where,  $H_s$  is the significant wave height and  $L_z$  is the wavelength corresponding to the zero-crossing frequency  $\omega_z = \sqrt{\gamma_2/\gamma_0}$  and  $\gamma_n$  is given by

$$\gamma_n = \int \omega^n S(\omega) d\omega \quad (5.6)$$



**Figure 11. Different criteria for  $ka$  as a function of  $kd$**

- **Stansberg [15]:** Stansberg proposed a useful criterion to establish the highest frequency, for which the second-order wave theory may be considered valid, as follows:

$$k_{cut} = \frac{2}{E(a_{max})[1 + 1/2(k_p E(a_{max}))]} \quad (5.7)$$

where  $k_{cut}$  is related to the limiting (cut-off) frequency,  $\omega_{cut}$ , through the linear dispersion relation and  $k_p$  is a wavenumber corresponding to the spectral peak period,  $T_p$ ;  $E(a_{max})$  is the expected value of the extreme wave amplitude of a gaussian wave record, which follows Rayleigh distribution. The denominator in Eq.5.7 is the simplified second-order correction for a non-gaussian wave field. According to the extreme value theory,  $E(a_{max})$  is given by

$$E(a_{max}) = \frac{H_s}{4} \left[ \sqrt{2 \ln(N_z)} + \frac{\gamma_{em}}{\sqrt{2 \ln(N_z)}} \right] \quad (5.8)$$

$$N_z = \frac{t_{max}}{T_z} \quad (5.9)$$

where,  $\gamma_{em} = 0.577\dots$  is the Euler-Meschenori constant;  $N_z$  is the number of zero-upcrossing wave cycles and  $t_{max}$  is the length of simulation in *sec*.

- **DNV-RP-C205 [16]:** DNV-RP-C205 guideline provides a simpler criterion for the application of second-order wave theory as follows:

$$\omega_{cut} = \sqrt{\frac{2g}{H_s}} \quad (5.10)$$

In irregular wave case, the validity of second order wave theory is significantly affected by the spectral or statistical properties of the considered irregular wave such as the peak wave period( $T_p$ ), significant wave height( $H_s$ ), and the length of simulation( $t_{max}$ ) depending on the considered criteria. During a numerical simulation of the second-order wave kinematic, therefore, the maximum wave frequency arbitrarily assigned without considering the spectral properties of the irregular wave may result in the generation of physically-incorrect second-order wave kinematics.

## 5.2 Sampling Theorem and additional requirement of cut-off frequency, $\omega_{cut}$

In digital simulation of wave surface elevation and kinematics, we replace continuous time  $t$ , by discrete time array,  $t_p = p\Delta t$ , where  $\Delta t = t_{max}/N$ , such that  $p = 1, 2, \dots, N$ . By virtue of the periodicity of Fourier series, we have

$$\Delta\omega = \frac{2\pi}{t_{max}} \quad (5.11)$$

The Nyquist sampling theorem provides a prescription for the nominal sampling interval required to avoid aliasing. It may be stated simply as follows:

- The sampling frequency,  $\omega_s = 2\pi/\Delta t$  should be at least twice the highest frequency contained in the signal.

Or in mathematical term,

$$\omega_s \geq 2\omega_{cut} \quad (5.12)$$

If  $\omega_{cut} = M\Delta\omega$ , then we must satisfy

$$\left[ \omega_s = \frac{2\pi}{\Delta t} = \frac{2\pi}{t_{max}/N} \right] \geq \left[ 2\omega_{cut} = M\Delta\omega = M\frac{2\pi}{t_{max}} \right] \quad (5.13)$$

$$\Rightarrow N \geq 2M \quad (5.14)$$

In the numerical simulation of second-order wave kinematics, the largest frequency of wave components generated by the second-order wave-wave interaction is  $2M\Delta\omega$ , which is associated with the sum-frequency interaction. Therefore, to satisfy the sampling theorem for second-order wave simulation, we must ensure that

$$N \geq 4M \quad (5.15)$$

This simply means that a cut-off frequency,  $\omega_{cut}$  evaluated by a criterion presented in sec.5.1 must satisfy

$$\left[ N = \frac{t_{max}}{\Delta t} \right] \geq \left[ 4M = 4\frac{\omega_{cut}}{\Delta\omega} = 4\frac{\omega_{cut}}{2\pi/t_{max}} \right] \quad (5.16)$$

$$\Rightarrow \omega_{cut} \leq \frac{\pi}{2\Delta t} \quad (5.17)$$



## 5.3 Numerical Simulation using Inverse Fast Fourier Transform(IFFT)

As shown in Eq.4.11 - Eq.4.36, the second-order wave kinematics can be obtained using the double Fourier transform. Although computation efficiency is improved by using IFFT, the formulations of the second-order wave kinematics are still time consuming. When the wave spectrum is divided into  $N$  components, the integration should be repeated  $N^2$  times, if direct integration method is applied. Fortunately, by collecting same frequency terms first, it is possible to reduce the calculation times to  $2N - 1$  for sum frequency contributions, and  $N - 1$  for difference frequency terms.

Figure 12 and 13 shows which second-order wave frequency is generated by sum and difference interaction between  $\omega_n$  and  $\omega_m$ . In the figure,  $\omega_1 = \Delta\omega$ ,  $\omega_2 = 2\Delta\omega$ ,  $\dots$ ,  $\omega_N = N\Delta\omega$ . If same frequency terms, i.e. the diagonal going from the lower left corner to the upper right corner in sum-frequency matrix and the diagonal going from upper left corner to the lower right corner in difference-frequency matrix, are collected, the double summation of  $N \times N$  terms can be replaced with a single summation of  $2N - 1$  terms for sum-frequency components ( $\omega_{\mu^+} = \mu^+\Delta\omega$ ;  $\mu^+ = \{2, 3, \dots, 2N\}$ ) and  $N - 1$  terms for difference-frequency components ( $\omega_{\mu^-} = \mu^-\Delta\omega$ ;  $\mu^- = \{1, 2, \dots, N - 1\}$ )

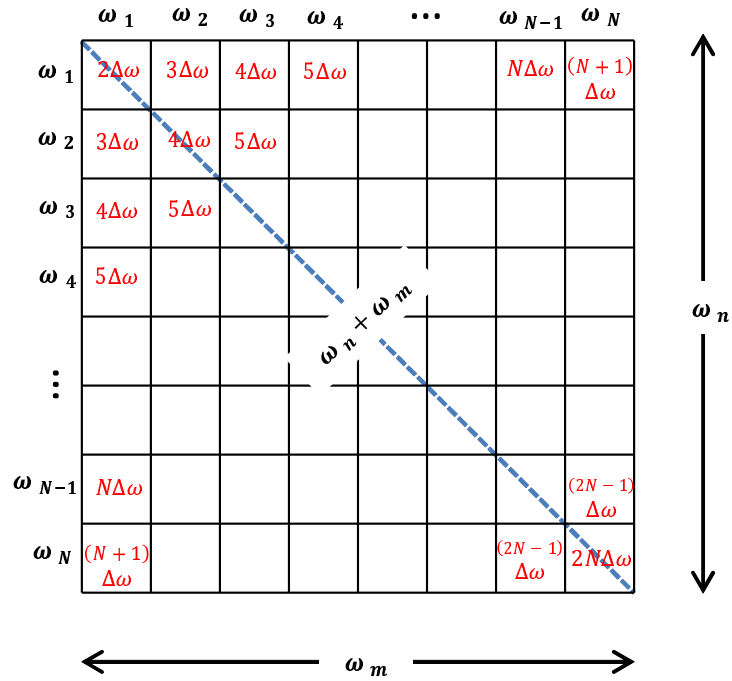


Figure 12. Second-order wave frequency matrix: Sum-frequency interaction

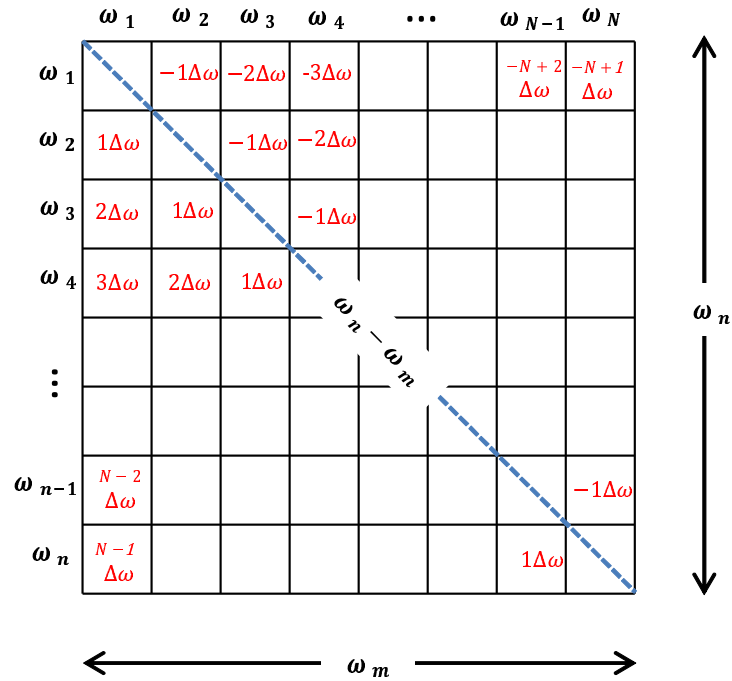


Figure 13. Second-order wave frequency matrix: difference-frequency interaction

### 5.3.1 Sum-Frequency Interaction

To simplify the computation of the sum-frequency wave kinematics, the matrix should be split into three regions:

- Region1 -  $n = m$ :  $\omega_{\mu^+} = \{2, 4, 6, \dots, 2N\} \times \Delta\omega$
- Region2 -  $n \neq m$  and  $3 \leq n + m \leq N + 1$ :  $\omega_{\mu^+} = \{3, 4, 5, \dots, N + 1\} \times \Delta\omega$
- Region3 -  $n \neq m$  and  $N + 2 \leq n + m \leq 2N - 1$ :  $\omega_{\mu^+} = \{N + 2, 4, 5, \dots, 2N - 1\} \times \Delta\omega$

Using the symmetricity property of QTFs introduced in sec.4.5.1, we can obtain the following equation for Fourier coefficient of sum-frequency interaction term,  $H_{\mu^+}$ :

- **Region1:**  
 $H_{\mu^+} = A_k A_k X^+(\omega_k, \omega_k)$  where  $\mu^+ = 2k$ ;  $k = \{1, 2, \dots, N\}$
- **Region2:**  
 $H_{\mu^+} = 2 \sum_{l=1}^{\lfloor (\mu^+-1)/2 \rfloor} A_l A_{\mu^+-l} X^+(\omega_l, \omega_{\mu^+-l})$
- **Region3:**  
 $H_{\mu^+} = 2 \sum_{l=\mu^+-N}^{\lfloor (\mu^+-1)/2 \rfloor} A_l A_{\mu^+-l} X^+(\omega_l, \omega_{\mu^+-l})$

where  $\lfloor \bullet \rfloor$  represents the floor function and  $X^+$  in above equations is equivalent to the sum-frequency part of red text in Eq.4.19, 4.20, 4.21, 4.28, 4.29, 4.30, and 4.35). After evaluating Fourier coefficient  $H_{\mu^+}$ , we can get a time series of the second-order wave kinematic,  $Y^+(\vec{x}, z, t)$  by applying one-dimensional IFFT procedure .

$$Y^+(\vec{x}, z, t) = IFFT [H_{\mu^+}] \quad (5.18)$$

### 5.3.2 Difference-Frequency Interaction

Unlike the sum-frequency interaction case, Fourier coefficient of difference-frequency interaction term,  $H_{\mu^-}$  can be evaluated a relatively simple equation without splitting the matrix as follows:

$$H_{\mu^-} = 2 \sum_{l=1}^{N-\mu^-} A_{l+\mu^-} A_l^* X^-(\omega_{l+\mu^-}, \omega_l) \quad (5.19)$$

where,  $\mu^- = \{1, 2, \dots, N - 1\}$ , and  $X^-$  in Eq.5.19 is equivalent to the difference-frequency part of red text in Eq.4.19, 4.20, 4.21, 4.28, 4.29, 4.30, and 4.35). By applying one-dimensional IFFT procedure, a time series of the second-order wave kinematic by difference wave-wave interaction is simply given

$$Y^-(\vec{x}, z, t) = IFFT [H_{\mu^-}] \quad (5.20)$$

## Bibliography

- [1] N. Sharma and R. Dean. Second-order directional seas and associated wave forces. *Society of Petroleum Engineers Journal*, 4:129–140, 1981.
- [2] G. G. Stokes. On the theory of oscillatory waves. *Trans.Camb. Phil. Soc.*, 8:441–455, 1847.
- [3] M.S. Longuet-Higgins, D.E. Cartwright, and N.D. Smith. Observations of the directional spectrum of sea waves using the motions of a floating buoy. In *Ocean Wave Spectra, Proceedings of the Royal Society of London. Series A, Mathematical and Physical Sciences*, 1963.
- [4] G.Z. Forristall. Kinematics of directionally spread waves. In *Proceeding on Directional Wave Spectra Applications, American Society of Civil Engineers*, 1981.
- [5] K.F. Lambrakos. Marine pipeline dynamic response to waves from directional wave spectra. *Ocean Engineering*, 9:385–405, 1982.
- [6] J.A. Pinkster. Numerical modelling of directional seas. In *Symposium on Description and Modelling of Directional Seas, Technical University of Denmark, Copenhagen*, 1984.
- [7] E.R. Jeffreys. Directional seas should be ergodic. *Journal of Applied Ocean Research*, 9:186–191, 1987.
- [8] M.D. Miles and E.R. Funke. A comparison of methods for synthesis of directional seas. *Journal of Offshore Mechanics and Arctic Engineering*, 111:43–48, 1989.
- [9] O.M. Faltinsen. *Sea Loads On Ships and Offshore Structures*. Cambridge University Press, 1990.
- [10] P.D. Scлавounos. *Ocean Wave Interaction with Ships and Offshore Energy Systems [lecture note]*. Retrieved from <http://bazzim.mit.edu/oeit/OcwWeb/Mechanical-Engineering/2-24Spring-2002/LectureNotes/index.htm/>. Massachusetts Institute of Technology, 2002.
- [11] C.-H. Lee. Wamit theory manual. Technical Report MIT Report 95-2, Department of Ocean Engineering, Massachusetts Institute of Technology, Cambridge, MA, 1995.
- [12] T. Marthinsen and S.R. Winterstein. On the skewness of random surface wave. In *Proceeding of the second international offshore and polar engineering conference*, 1992.
- [13] O. Nwogu. Nonlinear evolution of directional wave spectra in shallow water. In *Proceeding of Costal Engineering*, 1994.
- [14] S-L.J. Hu and D. Zhao. Non-gaussian properties of second-order random waves. *Journal of Engineering Mechanics*, 119:44–364, 1993.
- [15] C.T. Stansberg. Non-gaussian extremes in numerically generated second-order random waves on deep water. In *Proceeding of the Eighth international offshore and polar engineering conference*, 1998.
- [16] Det Norske Veritas. *Recommended practice - DNV-RP-C205 - Environmental conditions and environmental loads*. DNV, 2010.